Understanding the balance between methane production and oxidation from wetlands using a minimalistic emissions model: supplementary material

Gordon. R. McNicol, Anita. T. Layton, and Nandita. B. Basu

S1 Wetland drivers for P1, P3, P8, T3, T6, T9

In this Section we expand on Figs. 3–4 in the main text. In particular, we illustrate how emissions for each of these wetlands are driven by water table depth, soil temperature and carbon substrate availability (based on a lagged-NDVI term), based on data from Bansal and Tangen (2022); Bansal et al. (2023). These results are displayed for wetland P1 (Fig. S1), P3 (Fig. S2), P8 (Fig. S3), T5 (Fig. S4), T6 (Fig. S5) and T9 (Fig. S6), respectively, with optimised parameters based on Table 1 in the main text. Panels (a) and (b) from each of these figures feature in the main text in Figs. 3–4 of the main text.

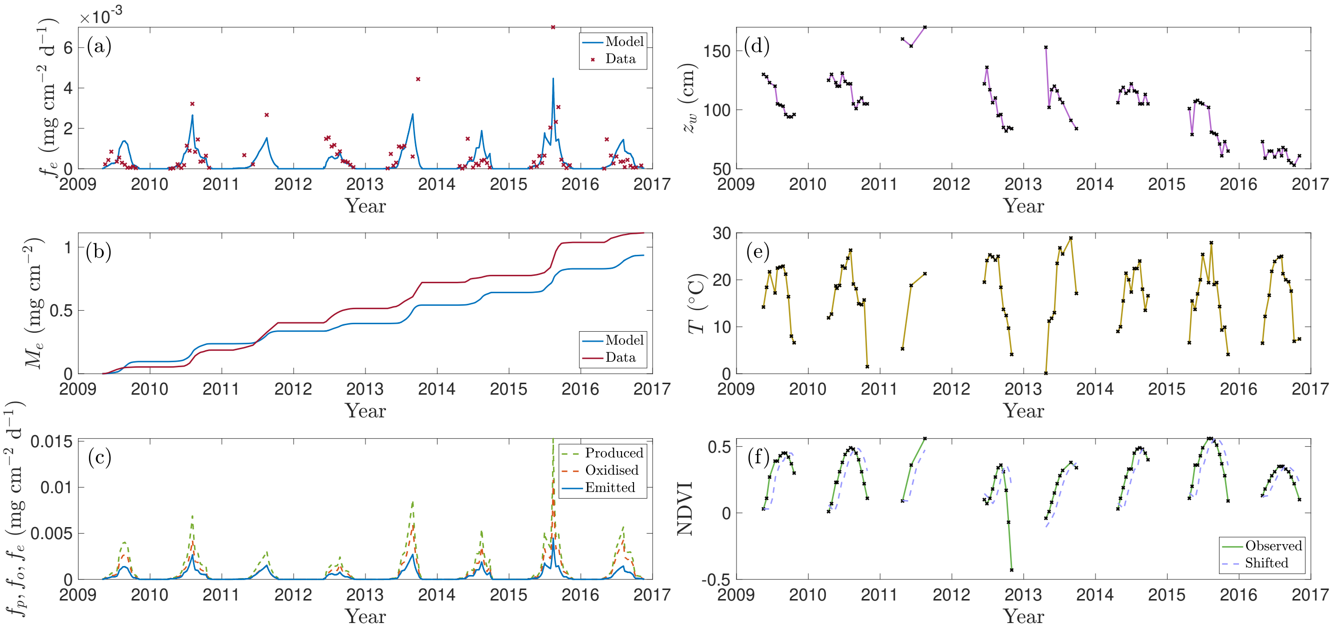

Figure S1: Baseline predictions for the centre of the P1 wetland. Panel (a) shows the modelled (blue line) and observed (red crosses; based on data from Bansal and Tangen, 2022) CH_4 fluxes over the growing seasons 2009–2016, the associated cumulative CH_4 emissions from the solver (blue line) and approximated from integration of the data (red line) are shown in panel (b). The rate of CH_4 production and oxidation in the soil column and CH_4 emissions from the soil column are summarised in panel (c). Each of these model predictions are forced by the drivers water table depth (panel d), temperature (panel e) and NDVI (panel f). Crosses in panels (d–f) reflect observed data, whilst lines show interpolated data between data points. The shifted NDVI used to infer the available carbon substrate for methanogenesis is shown by the dashed line in panel (f).

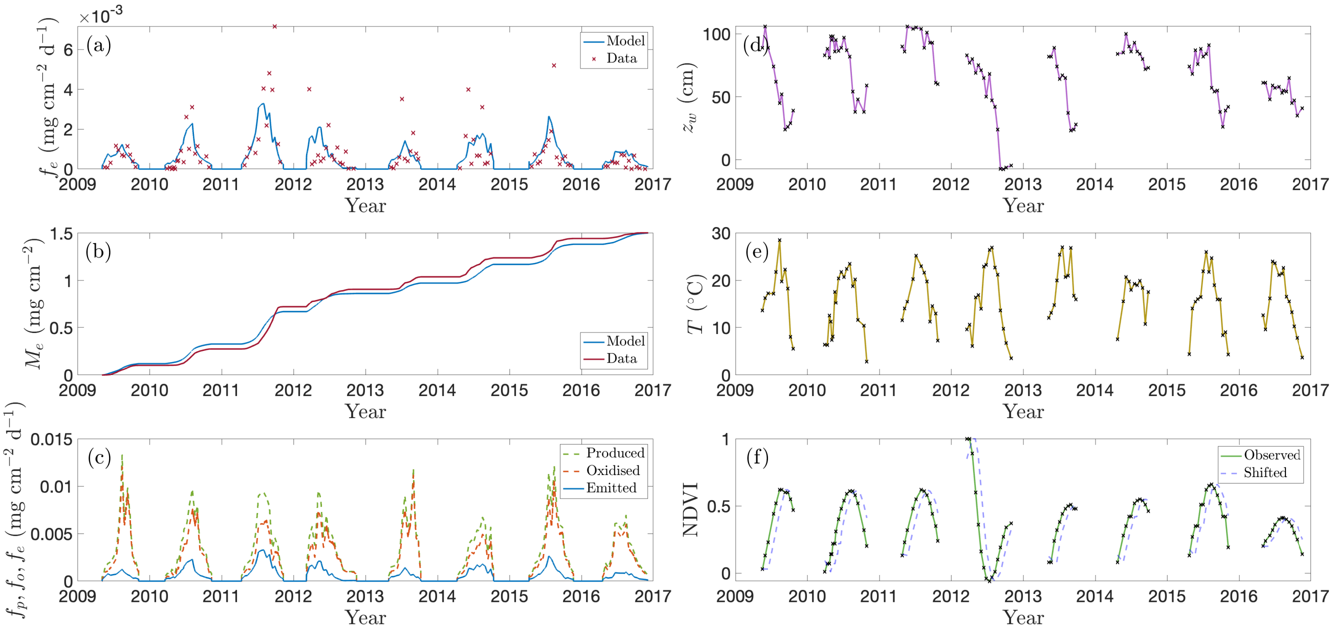

Figure S2: Baseline predictions for the centre of the P3 wetland. Panel (a) shows the modelled (blue line) and observed (red crosses; based on data from Bansal and Tangen, 2022) CH_4 fluxes over the growing seasons 2009–2016, the associated cumulative CH_4 emissions from the solver (blue line) and approximated from integration of the data (red line) are shown in panel (b). The rate of CH_4 production and oxidation in the soil column and CH_4 emissions from the soil column are summarised in panel (c). Each of these model predictions are forced by the drivers water table depth (panel d), temperature (panel e) and NDVI (panel f). Crosses in panels (d–f) reflect observed data, whilst lines show interpolated data between data points. The shifted NDVI used to infer the available carbon substrate for methanogenesis is shown by the dashed line in panel (f). Optimised parameters are detailed in Table 1 of the main text.

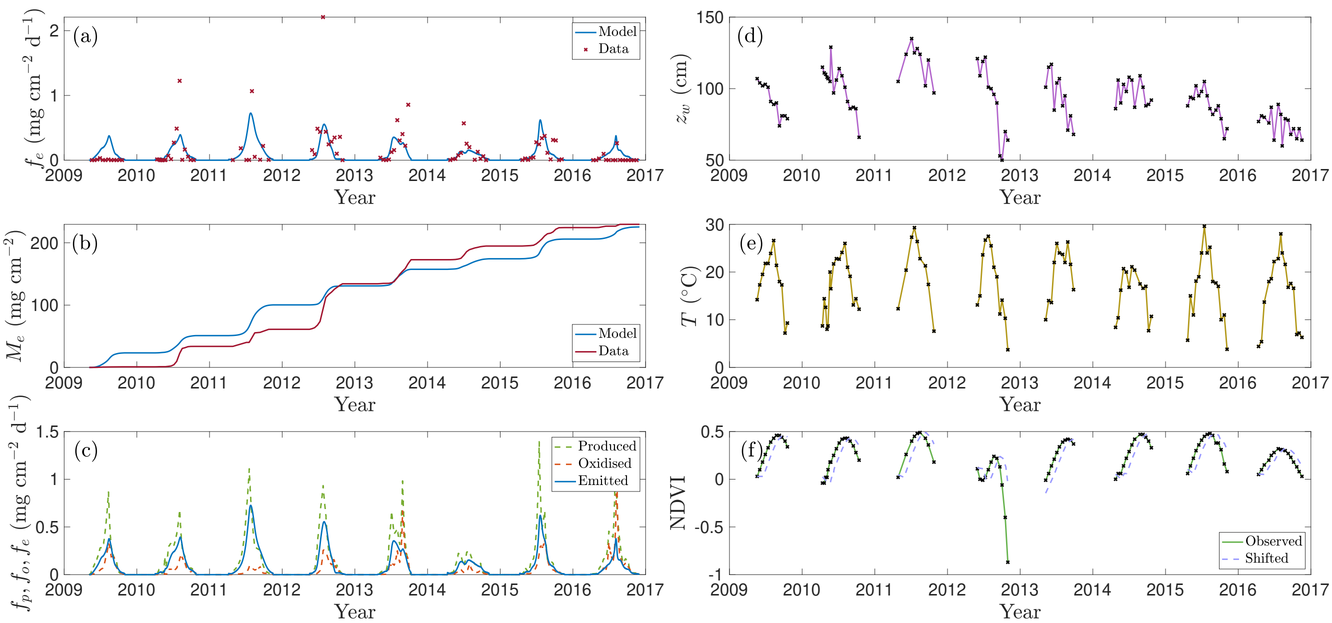

Figure S3: Baseline predictions for the centre of the P8 wetland. Panel (a) shows the modelled (blue line) and observed (red crosses; based on data from Bansal and Tangen, 2022) CH_4 fluxes over the growing seasons 2009–2016, the associated cumulative CH_4 emissions from the solver (blue line) and approximated from integration of the data (red line) are shown in panel (b). The rate of CH_4 production and oxidation in the soil column and CH_4 emissions from the soil column are summarised in panel (c). Each of these model predictions are forced by the drivers water table depth (panel d), temperature (panel e) and NDVI (panel f). Crosses in panels (d–f) reflect observed data, whilst lines show interpolated data between data points. The shifted NDVI used to infer the available carbon substrate for methanogenesis is shown by the dashed line in panel (f).

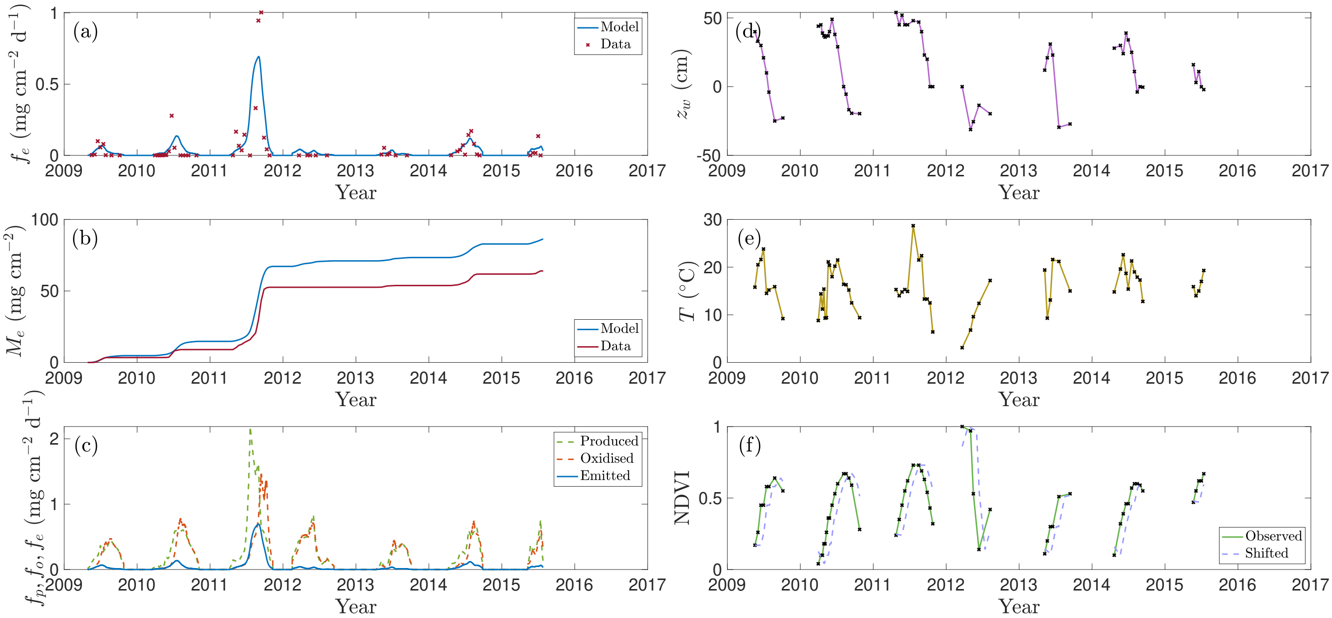

Figure S4: Baseline predictions for the centre of the T5 wetland. Panel (a) shows the modelled (blue line) and observed (red crosses; based on data from Bansal and Tangen, 2022) CH_4 fluxes over the growing seasons 2009–2016, the associated cumulative CH_4 emissions from the solver (blue line) and approximated from integration of the data (red line) are shown in panel (b). The rate of CH_4 production and oxidation in the soil column and CH_4 emissions from the soil column are summarised in panel (c). Each of these model predictions are forced by the drivers water table depth (panel d), temperature (panel e) and NDVI (panel f). Crosses in panels (d–f) reflect observed data, whilst lines show interpolated data between data points. The shifted NDVI used to infer the available carbon substrate for methanogenesis is shown by the dashed line in panel (f).

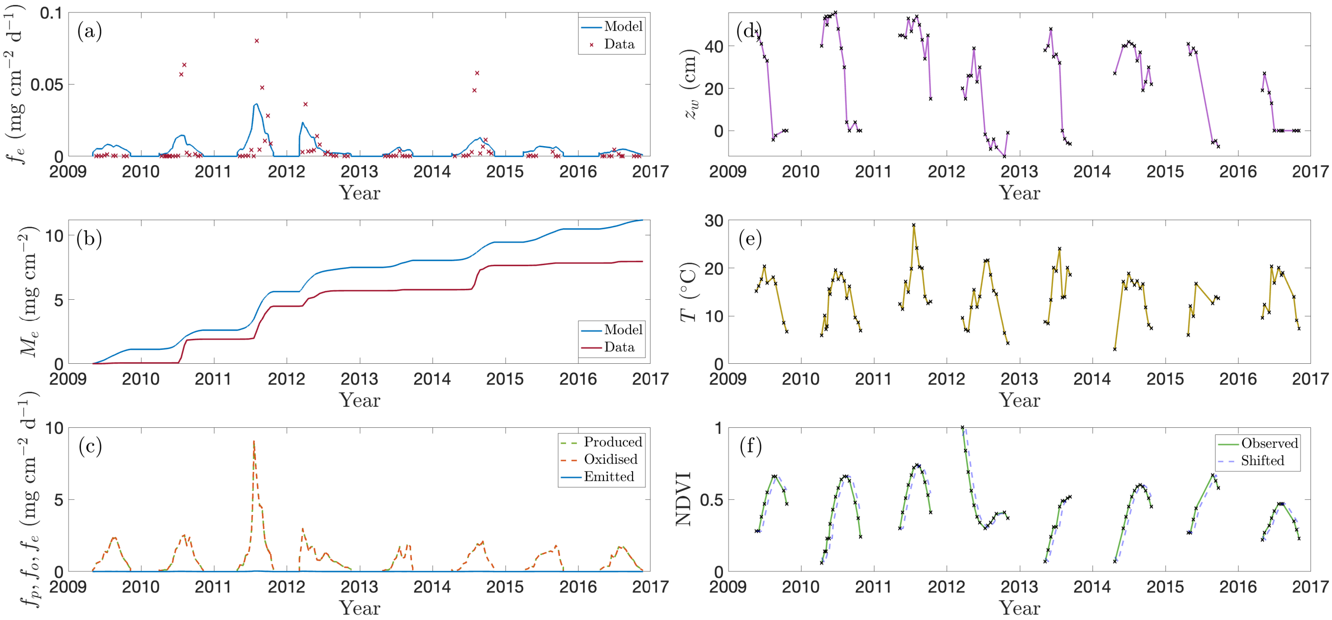

Figure S5: Baseline predictions for the centre of the T6 wetland. Panel (a) shows the modelled (blue line) and observed (red crosses; based on data from Bansal and Tangen, 2022) CH_4 fluxes over the growing seasons 2009–2016, the associated cumulative CH_4 emissions from the solver (blue line) and approximated from integration of the data (red line) are shown in panel (b). The rate of CH_4 production and oxidation in the soil column and CH_4 emissions from the soil column are summarised in panel (c). Each of these model predictions are forced by the drivers water table depth (panel d), temperature (panel e) and NDVI (panel f). Crosses in panels (d–f) reflect observed data, whilst lines show interpolated data between data points. The shifted NDVI used to infer the available carbon substrate for methanogenesis is shown by the dashed line in panel (f).

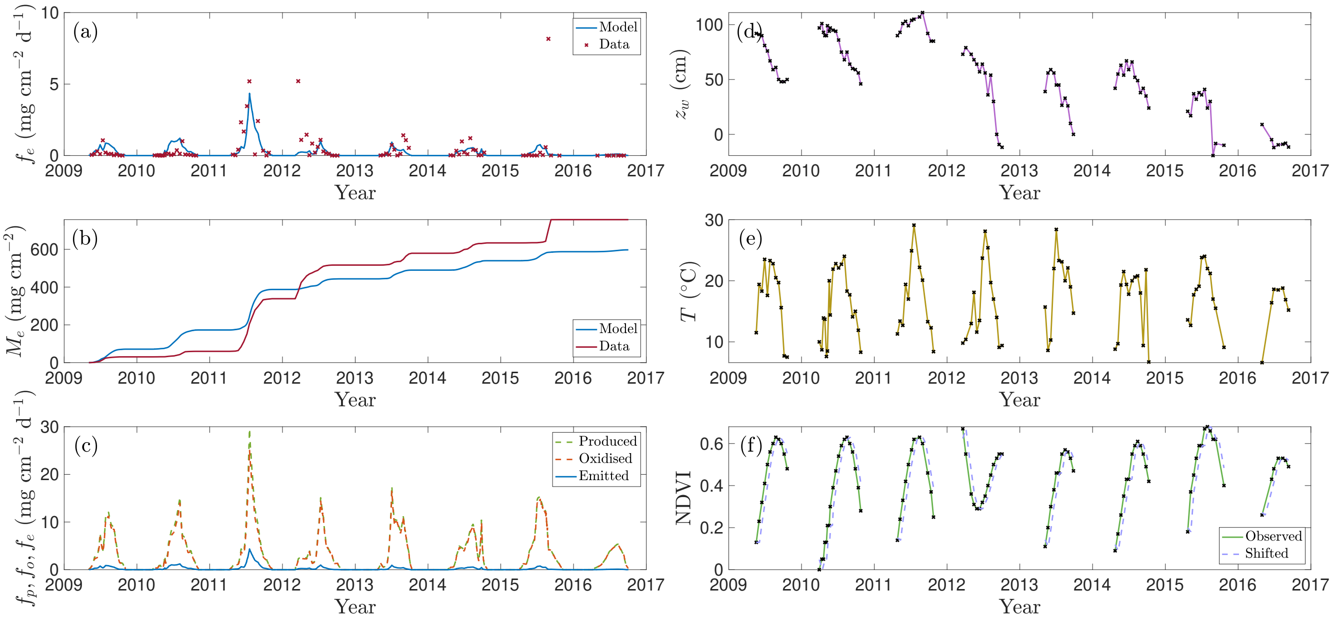

Figure S6: Baseline predictions for the centre of the T9 wetland. Panel (a) shows the modelled (blue line) and observed (red crosses; based on data from Bansal and Tangen, 2022) CH_4 fluxes over the growing seasons 2009–2016, the associated cumulative CH_4 emissions from the solver (blue line) and approximated from integration of the data (red line) are shown in panel (b). The rate of CH_4 production and oxidation in the soil column and CH_4 emissions from the soil column are summarised in panel (c). Each of these model predictions are forced by the drivers water table depth (panel d), temperature (panel e) and NDVI (panel f). Crosses in panels (d–f) reflect observed data, whilst lines show interpolated data between data points. The shifted NDVI used to infer the available carbon substrate for methanogenesis is shown by the dashed line in panel (f).

References

Bansal, S., Post van der Burg, M., Fern, R.R., Jones, J.W., Lo, R., McKenna, O.P., Tangen, B.A., Zhang, Z., Gleason, R.A., 2023. Large increases in methane emissions expected from north america's largest wetland complex. Sci. Adv. 9, eade1112. doi:10.1126/sciadv.ade1112.

Bansal, S., Tangen, B., 2022. Methane flux model for wetlands of the prairie pothole region of north america: Model input data and programming code. U.S. Geological Survey data release. URL: `https://doi.org/10.5066/P9PKI29C`, doi:10.5066/P9PKI29C.